ADVANCED FUNCTIONAL MATERIALS
www.afm-journal.de

Doping Rules and Doping Prototypes in A_2BO_4 Spinel Oxides

*Tula R. Paudel, Andriy Zakutayev, Stephan Lany, Mayeul d'Avezac, and Alex Zunger**

A_2BO_4 spinels constitute one of the largest groups of oxides, with potential applications in many areas of technology, including (transparent) conducting layers in solar cells. However, the electrical properties of most spinel oxides remain unknown and poorly controlled. Indeed, a significant bottleneck hindering widespread use of spinels as advanced electronic materials is the lack of understanding of the key defects rendering them as p-type or n-type conductors. By applying first-principles defect calculations to a large number of spinel oxides the major trends controlling their dopability are uncovered. Anti-site defects are the main source of electrical conductivity in these compounds. The trends in anti-sites transition levels are systemized, revealing fundamental "doping rules", so as to guide practical doping of these oxides. Four distinct doping types (DTs) emerge from a high-throughput screening of a large number of spinel oxides: i) donor above acceptor, both are in the gap, i.e., both are electrically active and compensated (DT-1), ii) acceptor above donor, and only acceptor is in the gap, i.e., only acceptor is electrically active (DT-2), iii) acceptor above donor, and only donor is in the gap, i.e., only donor is electrically active (DT3), and iv) acceptor above donor in the gap, i.e., both donor and acceptor are electrically active, but not compensated (DT-4). Donors and acceptors in DT-1 materials compensate each other to a varying degree, and external doping is limited due to Fermi level pinning. Acceptors in DT-2 and donors in DT-3 are uncompensated and may ionize and create holes or electrons, and external doping can further enhance their concentration. Donor and acceptor in DT-4 materials do not compensate each other, and when the net concentration of carriers is small due to deep levels, it can be enhanced by external doping.

1. Introduction

A_2BX_4[1] spinels (X = O, S, Se, Te)[2,3] comprise a broad group of chalcogenides containing two metal atoms (A and B), being either III-valent and II-valent cations (giving the III_2-II-VI_4 spinel group,e.g., Al_2MgO_4) or II-valent and IV-valent cations (giving the II_2-IV-VI_4 spinel group,e.g., Cd_2SnO4. There are about 1000 known spinels including ~130 oxides, some of them explored previously for ferroelectricity,[4] ferromagnetism,[5] superconductivity,[6] thermoelectricity,[7–10] and catalytic properties.[11,12] Only recently this large group of materials has been tapped for its potential in electronic and optoelectronic applications.[13–16] Such applications would require first and foremost that these materials can be doped n-type and/or p-type, even though the perfectly stoichiometric III_2-II-VI_4 or II2-IV-VI_4 systems generally form a closed-shell octet, and hence tend to be insulators.

It is important to realize that doping in spinels can follow different rules from doping in traditional electronic materials, such as Si or GaAs. The main reasons are that (a) spinels have both octahedral and tetrahedral occupied cation sites, and (b) that spinels often contain multivalent elements such as transition metal ions. These ions (can) switch their valence when moved from one coordination to another, and such a change in valence may lead to hyperdeep electrical levels such as donors inside the valence band and acceptors inside the conduction band. This is in contrast to the traditional semiconductors, in which acceptor levels usually lie in the lower part of the gap and donor levels usually lie in the upper part of the gap. Thus the doping physics of spinels is more difficult and interesting compared to conventional semiconducting materials.

Dr. T. R. Paudel, Dr. A. Zakutayev, Dr. S. Lany, Dr. M. d'Avezac
National Renewable Energy Laboratory Golden
CO 80401, USA
Prof. A. Zunger
University of Colorado
Boulder, CO 80309, USA
E-mail: alex.zunger@gmail.com

DOI: 10.1002/adfm.201101469

1.1. Recent Work on Spinel Doping

Previous experimental[13,15–26] and theoretical attempts[22,27–31] to study doping of such oxides have revealed one interesting feature: even when a would-be dopant is successfully introduced, the Fermi level is often pinned in a narrow energy region in the gap and would not shift much when more dopants are added. Therefore, sightings of spinels that manifest some free carriers when off-stoichiometric or intentionally doped have been sporadic[13–15,18,20,32–38] and unpredictable. Indeed, the type of conductivity (n or p or neither), and far more its magnitude, of the vast majority of spinels is still unknown, this being a major impediment for their

© 2011 WILEY-VCH Verlag GmbH & Co. KGaA, Weinheim

exploitation as electronic materials. Attempts have been previously made[13–15] to distill some phenomenological expectations from the few known examples, establishing what makes a spinel n- or p- type. It was thought that (i) oxygen vacancy V(O) is the cause of n-type conductivity,[14,15,37] as supported by the fact that oxygen deficiency is correlated with electron conductivity, and that (ii) cation vacancy V(A) or V(B) is the cause of p-type conductivity, as supported by the general knowledge that cation vacancies are usually acceptors. Concomitantly, it was thought that (iii) excess of the high-valent cation (e.g., III in III_2-II-VI_4) will enhance n-typeness and defeat p-typeness[28,39] of a spinel because III-on-II substitution is expected to be an electron-producing (hole-killing) donor. iii) Interstitial defects in the closed pack spinel structure are tought to be unlikely and hence do not affect its electrical properties.[40,41] Extra cation in an interstitial position lead to metal–metal bonding or metal–oxygen underbonding,[42] hence energetically they are difficult to form. These phenomenological principles have been guiding the search and optimization of doped spinels, but with little success. Previous first-principle calculations[22,28] were limited to a few specific compounds, and no attempts have been made so far to extract general understanding and general rules of doping in this family of oxides.

1.2. Present Realizations

Using an extensive set of first-principles calculations of defect formation energies, ionization levels, and carrier concentration as a function of temperature and oxygen pressure, we found a different physical picture, namely that the anti-sites are much more abundant in spinels than the vacancies or interstitials. This finding implies different practical design principles to guide doping in spinels.

i) Oxygen vacancies are not the leading cause of n-type conduction in most of the spinels, nor are cation vacancies the leading cause of p-type conduction. Generally, oxides differ greatly in their propensity to form oxygen vacancies. For example, ZnO is an oxide having as many as 10^{19} cm^{-3} oxygen vacancies in favorable oxygen-poor (reducing) conditions.[43] In contrast, the absolute majority of the typical spinels shown in **Figure 1** have less than 10^{16} cm^{-3} oxygen vacancies even in reducing condition, as predicted by the formation energy of the defect calculated using the first principles and the thermodynamic simulations assuming the thermal equilibrium and taking into account the configurational entropy that arises due to different ways of arranging the defects among the available number of sites. The only exceptions in Figure 1 that do manifest a high concentration of V(O), comparable to the concentration of anti-site donors are Ga_2ZnO_4 and Cr_2MnO_4 but the corresponding donor levels are energetically deep so oxygen vacancy is not the leading cause of n-type conductivity, even in these two spinel oxides (for example, the V(O) is double donor (0/2+) meaning the energy where V(O) changes from having charge $q = 0$ to $q = +2$ in Ga_2ZnO_4 and it occurs at $E_c - 2.4$ eV, whereas in Cr_2MnO_4 its a single donor (0/1+) meaning the energy where V(O) changes from having charge $q = 0$ to $q = +1$ and it occurs at $E_c - 2.8$ eV, with E_c being the short-hand notation for conduction band minimum). Similar to the oxygen vacancy, cation vacancies are not the leading source of p-type behavior, as can be seen from the survey of V(A) and V(B) vacancy concentrations in Figure 1. In a few spinels, such as Fe_2FeO_4, it has been shown experimentally that oxygen vacancies are not the main defects.[44,45] Since oxygen, cation vacancies, and interstitial defects are not the

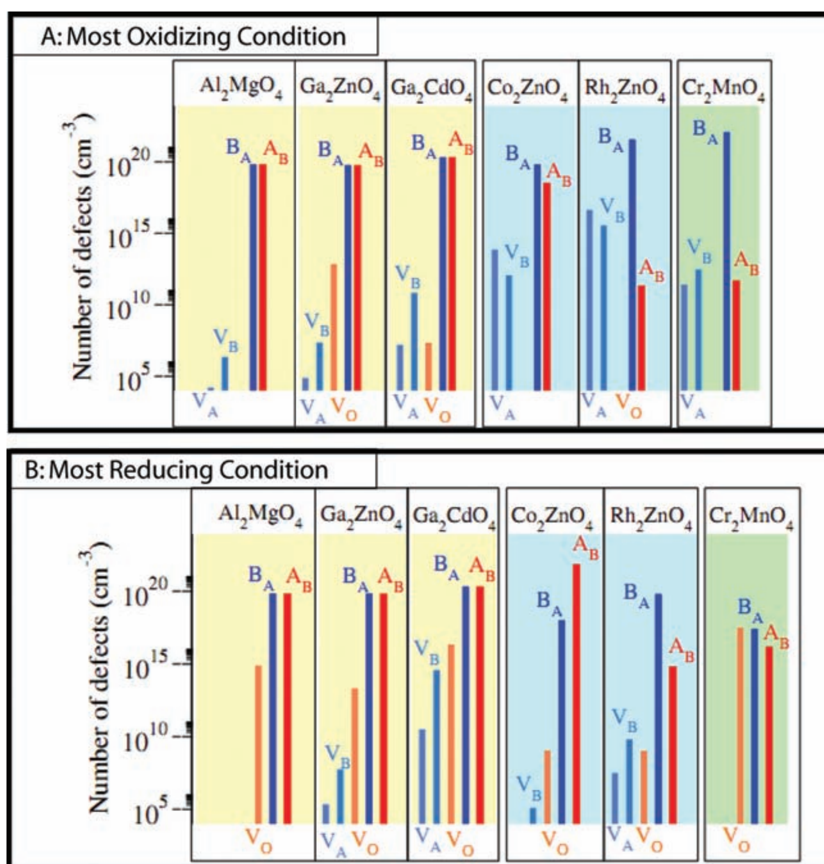

Figure 1. Showing the number of defects (logarithmic scale) of A, B, and O vacancies compared to number of anti-sites defects. The top panel (A) corresponds to the the most oxidizing condition (compound to be in equlibrium with binary oxides of B cation) and the bottom panel (B) to the most reducing condition at a typical growth temperature of 700 °C. It is to be noted that the most oxidizing condition where in most of cases the compound exist in equilibrium with the oxgyen molecule is very hard to realize. In such oxidizing conditions cation-related defects in some compounds such as Rh_2ZnO_4 and Cr_2MnO_4 become comparable with the donor type A-on-B anti-site defects, however overall defect physics remain dominated by acceptor type anti-site B-on-A. Further, not every compound exist in reducing condition such that they are in equilibrium with one or both of the metallic cations. For example, the Co_2ZnO_4 in the maximally reducing condition is limited by formation of Co_3O_4 and ZnO, where as for other compounds it is limited by formation of one or both of the metal ions.

© 2011 WILEY-VCH Verlag GmbH & Co. KGaA, Weinheim

main defects that control the dopability of spinel oxides, they will not be discussed further in this paper.

ii) Metal-on-metal anti-site substitutions are the leading cause of atomic disorder in spinel. Figure 1 illustrates this doping principle, showing that generally metal anti-sites are more prevalent than vacancies. One possible reason is that both cations in spinels have similar orbital radii,[2] and therefore it is energetically less costly to substitute one cation by the other and emit or absorb a carrier than to create a metal vacancy and to repair broken bonds. In the most oxidizing condition, in compound like Rh_2ZnO_4 and Cr_2MnO_4 (where the most oxidizing condition is defined by Rh_2ZnO_4 to be in equilibrium with RhO_2 and ZnO, and Cr_2MnO_4 to be in equilibrium with Mn_3O_4 and Cr_2O_3), cation vacancies becomes comparable with donor-type anti-site defects, A-on-B. However such an oxidizing condition is difficult to realize in practice, and even if one manages to achieve such condition by applying external pressure, then the overall defect is dominated by acceptor-type anti-site B-on-A. However, typically these compounds are grown often at higher temperature using binaries rather then the oxygen molecules and metallic ions.[20,46] In such conditions the number of cation vacancies decreases and anti-site defects becomes dominant as can be seen in Figure 1B. When the respective anti-site ionization levels reside in the band gap, cation anti-site is also the main promoters of conductivity. Cation anti-sites will be discussed in greater detail below.

These two new and surprising rules that emerge from this study open the way to deliberate design and discovery of novel electronic materials from the large and previously untapped group of spinels. For example, we have shown that engineered excess of the lower-valent cation (e.g., II in III_2-II-VI_4) enhances p-typeness in one class of spinels (for example Rh_2ZnO_4 and Co_2ZnO_4[47]), whereas it has practically no effect in other classes of spinels (for example Al_2MgO_4). This difference reflects the tendency of the donor level associated with substitution of the high-valent cation on the site of the low-valent cation to be inside the valence band (Co_2ZnO_4 and Rh_2ZnO_4), deep in the band gap (Cr_2MnO_4), or shallow in the band gap but compensated by a shallow acceptor (Al_2MgO_4). We will explain these spinel doping rules by means of detailed calculations in the rest of this paper.

2. Methods of Calculation

We have used the supercell approach within the density functional theory (DFT) to calculate for 40 A_2BO_4 spinel compounds:

i) The formation enthalpy $\Delta H(E_F,\mu)$ of various point defects as a function of the Fermi energy E_F in the band gap and the chemical potential μ of the constituent elements

ii) the associated acceptor and donor transition energies $E(q/q')$ between charge states q and q', (cf., Figure 4, Figure 5, and Figure 6 in Section 3.4. and 3.5);

iii) the defect concentration (c.f. Figure 1)

iv) the equilibrium Fermi energy $E_F(T,\mu)$. The method of calculating the formation energy is described by Lany and Zunger[48] and that for calculating equilibrium Fermi energy and defect concentration has been described in detail by Biswas et al.[49] The method that is used to calculate the formation energy has been tested in serveal cases,[50–54] including ZnO and GaAs,[48,55] In_2O_3,[56] and Cu_2O.[57]

In the following we discuss briefly how each of aforementioned quantities is computed including the correction beyond standard DFT total energy calculations.

2.1. Calculation of the Formation Enthalpy

To calculate the formation energy in supercell approach, one first considers a system in thermodynamic equilibrium with the reservoir, with which it exchanges atoms to create defects. Then the formation energy of a neutral defect can be calculated as the sum of energy difference between total energy of a supercell with a defect and without a defect, and the difference between the chemical potential of the removed and added atom. For the charged defect we further assume the system to be in equilibrium with the charge reservoir, i.e., the Fermi sea. We then add the chemical potential of an electron, i.e., the energy of Fermi sea E_F above the top of valance band maxima (VBM), when charges are removed from the system, as in the case of donors or subtract E_F, and when charges are added to the system, as in the case of the acceptors. The obtained formation energy of the charged defect has to be corrected.

i) Correction for the finite supercell size effect and potential alignment effect: To accurately calculate the formation energy for the charged defect in the limit of dilute defect concentration we explicitly calculate the contribution to the formation energy due to interaction of a charge with its image in the periodic system. We use the screened Madelung energy of a point charge compensated by a jellium background, as suggested by Leslie and Gillian,[58] and the extension due to Makov and Payne,[59] who suggested to include an additional term that account for the interaction between the delocalized part of defect-induced charges with the screened point-charge of images to fully take into account the interaction between charges and their periodic images. The dielectric constant that determines screening is calculated by using density functional perturbation.[60] Further, the reference potential between the cell containing the defect and the cell without a defect has been aligned explicitly considering the difference between the average potential at PAW radii in the defect-free host and defect-containing cell.

ii) The Moss–Burstein-type[61,62] band filling effect plays a role in the determination of the formation energy for both charged and neutral defect. This effect arises due to electrons occupying the bottom of the conduction band (CBM) instead of the donor level, and holes occupying the top of the valence band maxima (VBM) instead of the acceptor level. This effect is included by taking the difference between the sums of energy of the occupied bands above the host CBM and E_c or the unoccupied bands below the host VBM and E_v, including a potential-alignment effect in the full Brillouin zone, as described by Lany and Zunger.[48] It has been shown by Lany and Zunger[48,55] that formations energies calculated in the finite-size supercell, including aforementioned corrections, accurately represent the formation energy of a defect in infinite system.

© 2011 WILEY-VCH Verlag GmbH & Co. KGaA, Weinheim

2.2. Acceptor and Donor Transistion Energy

i) The associated acceptor and donor transition energie E(q/q′) between two charge states q and q′: Once the accurate formation energy is calculated for each charge state of a defect in a cell, the transition energy can be easily calculated by dividing the difference between the defect formation energies between two charge defects by their charge difference, as described by Paudel and Lambrecht.[63] We then correct the position of the transition levels taking into account the DFT band gap error GGA+U approximation.
ii) DFT band gap error: It is well known in DFT that the band gap is underestimated, as the valence band minimum (VBM) lies too high and the conduction band minimum (CBM) lies too low with respect to vacuum conditions. We correct the position of VBM to a large extent by adding Hubbard "U" to the transition metal d-orbital and approximate the CBM by introducing a-posteriori an arbitrary shift of 1 eV on the top of GGA+U CBM. The shift of the CBM by 1 eV represents the typical magnitude of the band gap underestimation of GGA+U calculations for the compounds considered in our work. This a-posteriori correction of CBM mostly affects shallow donors that are usually associated with the Moss–Burstein shift, as they are expected to follow CBM. Thus, we shift the transition levels of shallow donors along with the conduction band. Deep donors are left as calculated in the GGA+U level, as they are not expected to follow the CBM. Here, we would like to stress that the shift we employed for moving up CBM is unphysical. However no matter what the real band gap correction is, the deep transition levels are expected to remain the same, whereas shallow donors would move up in such a way that the difference between the band edge and the transition level will remain constant.

2.3. Defect Concentrations

Defect concentrations are calculated by minimizing the Gibbs free energy of defective cells with respect to the concentration of defects, assuming ΔH is independent of the defect concentration, and only the configurational entropy resulting from different ways of arranging defects among the available numbers of sites is taken into account. The defect concentrations (cf., Figure 1) at the equilibrium Fermi energy $E_F(T,\mu)$ in semiconductors is the function of number of carriers at a given temperature and chemical potential. The number of carriers is contributed by the ionized defects, which in-turn is determined by the position of the equilibrium Fermi energy $E_F(T,\mu)$. Hence, we calculate self-consistently the number of defects, the equilibrium Fermi energy $E_F(T,\mu)$, and the carrier density by requiring overall charge neutrality in the system as described by Biswas et al.[49]

Computational parameters: Density functional theory (DFT) band structure approach as implemented in VASP code[51,52] is used with PAW[53] and PBE pseudopotential.[54] Exchange and correlation effects beyond GGA are treated in a rotationally invariant GGA+U formalism,[55] with U determined in such a way that it correctly reproduces the relative stability of competing binaries.[56] Defect calculations are performed by a supercell approach. Our supercell consists of $N(A_2BO_4)$ cubic unit cells with $N = 8$ (a total of 56 atoms) and $2 \times 2 \times 2$ Monkhorst-Pack[56] k-points with a kinetic energy cutoff of 340 eV and oxygen soft pseudopotentials. In a few materials, such as Co_2ZnO_4, Rh_2ZnO_4, and Al_2MgO_4, we checked the convergence of the formation energy using 112 atom supercells including corrections and $4 \times 4 \times 4$ k-points and found the formation energy of a defect to converge within 0.01 eV.

3. Results

3.1. Structural Considerations

At T = 0 K A_2BX_4 spinels appear in either normal or inverse structural form. At low temperature, both normal and inverse spinels are found in ordered phase. In the ordered-normal phase (space group Fd3m) the A-cation (high–valent in–out notation) resides on the octahedral (O_h) site that is coordinated by six oxygen atoms, whereas the B-cation (low-valent in our notation) resides on the tetrahedral (T_d) site that is coordinated by four oxygen atoms. In this structure the system is a closed-shell insulator. In the ordered-inverse spinel (space group $P4_122$) the A-cation is distributed equally between the T_d and O_h sites, whereas all of the B-cation resides on the O_h site. It has recently been shown[64] that the preference between ordered-normal and ordered-inverse is determined by the "anion displacement parameter" u (obtainable from energy minimization or diffraction experiments), that also decides the position of oxygen atoms with respect to their neighboring cations.

At finite temperature, there are two different channels of disorder. The first is the configurational disorder with perfect stoichiometry: In this case the A:B:O ratio is still 2:1:4, but cations are swapped between O_h and T_d, as described by the general formula $[A_{2-\lambda} B_\lambda](A_\lambda B_{1-\lambda})O_4$ with an inversion parameter ($0<\lambda<1$), where λ defines the degree of inversion and square and round brackets denote [octahedral] and (tetrahedral) sites, respectively. This configurational entropy effect causes two different order–disorder phase transitions at perfect stoichiometry depending on the starting configuration: a) continuous transition between ordered-normal to disordered-dual (both Fd3m but λ increases from zero towards 2/3, creating B-on-O_h and A-on-T_d structures); b) first-order transition from ordered-inverse ($P4_122$) to disordered-inverse (Fd3m). Here λ stays 1 but the occupancy of the O_h sites get randomized. This is followed by second-order phase transition from the disordered-inverse to disordered-dual (both Fd3m but λ decreases from 1 towards 2/3). The second channel of disorder is change of stoichiometry, where the A:B:O ratio is altered from 2:1:4.

Both the cation disorder and the non-stoichiometry can cause doping in the materials. We focus on the doping, irrespective whether the compound is non-stoichiometric or stoichiometric with disorder in the cation sub-lattices at finite temperature.

3.2. Two broad doping classes: Compensated vs. Uncompensated Spinels

Our calculations show that doping behavior due to cross-substitutions can be classified into two broad groups that contain compensated and noncompensated defects (**Figure 2**), which

© 2011 WILEY-VCH Verlag GmbH & Co. KGaA, Weinheim

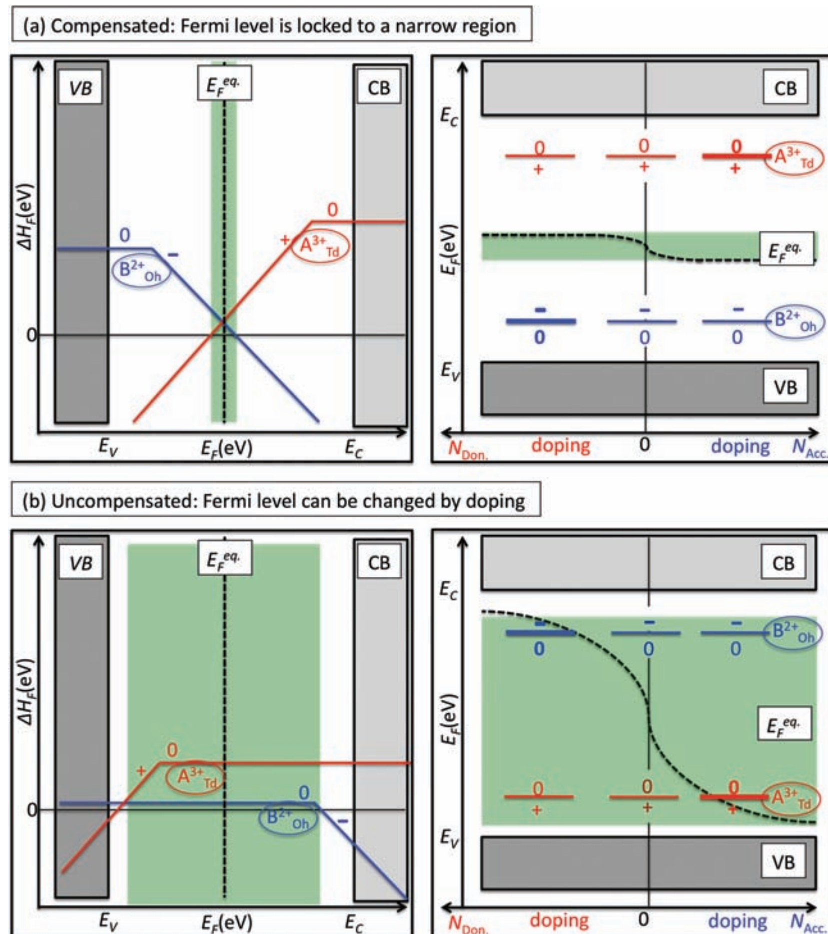

Figure 2. Two broad groups due to relative position of anti-site transition levels. In the first group (a), the Fermi level is pinned to a narrow region by a negative feedback mechanism, while in the second group (b) the movement of the Fermi level is unrestricted to a wide region. If donor level is below VBM, E_F can be moved all the way below VBM (good for p-type doping), similarly if the acceptor level is above CBM, E_F can be moved above CBM (good for n-type doping).

is further subdivided into four doping types, depending on the positions of the defect energy levels with respect to band edges (**Figure 3**). Compensated defects occur in materials where cross-substitution causes the donor level to be above the acceptor level (Figure 2a), and uncompensated defects occur when the acceptor level is above the donor level (Figure 2b). In the former case of donor-above-acceptor (Figure 2a), the Fermi energy can be pinned into a narrow range because of a negative feedback mechanism that counteracts intentional doping. We call materials with pinned Fermi level doping-type 1 (DT-1) materials. As shown in Figure 2a, right panel, in DT-1 materials, intentional n-type doping will initially shift the Fermi level *up* in the gap, causing an easier formation of native hole-producing acceptors such as B^{2+}-on-O_h due to lowering of their formation energy (and a less-easy formation of A^{3+}-on-T_d donors), thus shifting the Fermi energy *down* in the band gap. Conversely, intentional attempts of p-type doping of such a material would initially shift E_F *down* the gap, but this will cause the easier fromation of native electron-producing donors such as A^{3+}-on-T_d due to lowering of their formation energy (and a less-easy formation of B^{2+}-on-O_h acceptors), thus shifting the Fermi level *up* in the gap. External dopants will also behave similar as the intrinsic dopants. For example, adding external n-type dopants to the T_d site will shift E_F towards the CBM and thus cause formation of additional B^{2+}-on-O_h anti-site defects, but there is no requirement that an equal amount of A^{3+}-on-T_d would form. In fact, the Fermi level change in response to external n-type doping would even raise the formation energy of A^{3+}-on-T_d, thereby reducing their numbers. The shaded green region in Figure 2a, right panel illustrate the narrow range over which such pinning can occur in a material with comparable formation energy and transition levels of both donors and acceptors. Asymmetry in the energetic properties of defects may cause this narrow region to move closer to one of the band edges or even inside of the band, as will be discussed below in more details. In the case of acceptor-above-donor (Figure 2b, right panel), the Fermi level movement is essentially unrestricted. We call such materials doping-type 4 (DT-4) materials (see Figure 3). It is also possible that one defect is compensated and the opposite-charge defect is uncompensated. In these cases, the Fermi level movement is only partially restricted by either electrically active acceptors or electrically active donors. Such materials make good p-type or n-type semiconductors, and we call them doping-type 2 (DT-2) and doping-type 3 (DT-3) materials (see Figure 3), respectively. Four doping types of spinels are summarized in Figure 3 and will be discussed in more details in the following sections.

3.3. Heuristic Relation Between the Valence and the Electrical Character of Anti-Site-Substitution

The defect energy levels in Figure 3 are related to the ability of atoms to switch their valence when moved from their home base. The atoms that do switch their valence have extremely deep energy levels that are electrically neutral (for example donors in DT-2, acceptors in DT-3, or both in DT-4). The atoms that do not switch their valence have much shallower energy levels, capable of releasing electrons or holes and capable of compensating other charged defects (for example acceptors in DT-2, donors in DT-3, or both in DT-1). The chemical heuristics that decides the electrical character of the anti-site defect levels are based on the valence of atoms is as follows:

i) If the A-cation (which is high-valent on its O_h home-base in normal spinel) remains high-valent when it is moved from an O_h to a T_d site, then such cross-substitution to A^{3+}-on-T_d would lead to a donor level, capable of releasing electrons.
ii) Conversely, if A lowers its valence when it is moved from an O_h to a T_d site, then such a substitution to A^{2+}-on-T_d would be electrically neutral.
iii) Similarly, if the B-cation, (which is low-valent on its T_d home

© 2011 WILEY-VCH Verlag GmbH & Co. KGaA, Weinheim

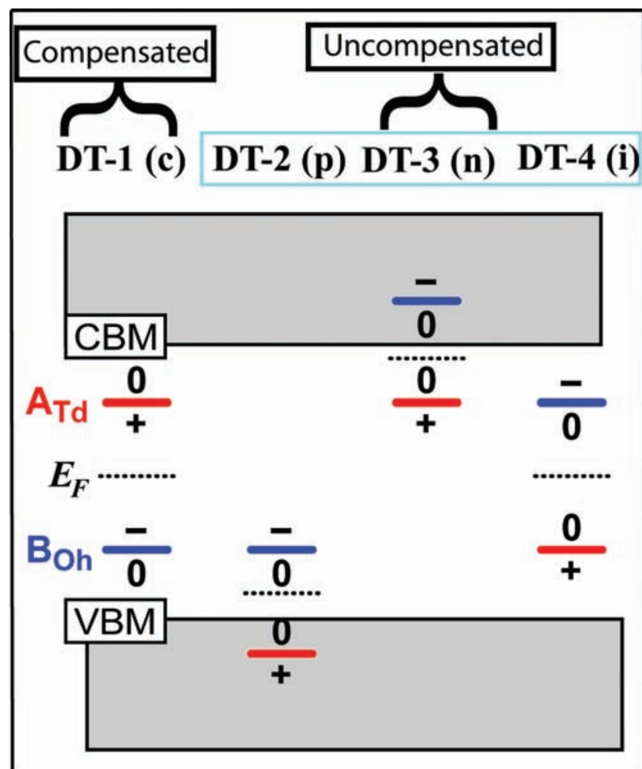

Figure 3. Schematic depiction of the energetic order of the donor A-on-T_d (red) and the acceptor B-on-O_h (blue). This leads to four DTs with doping characteristics being "compensated" (c), p-type (p), n-type (n), or intrinsic (i).

base in a normal spinel) remains low-valent when it is moved from a T_d to an O_h site, then such a substitution to B^{2+}-on-O_h could lead to an acceptor level, capable of releasing holes.

iv) Finally, if B raises its valence when it is moved from a T_d to an O_h site, then such substitution to B^{3+}-on-O_h will be electrically neutral.

In the remaining part of this paper we will use DFT calculations of the donor and acceptor levels without relying on the chemical heuristic rules stated above. If a donor transition levels falls into the valence band then it is electrically inactive. If an acceptor transition levels falls into the conduction band then it is also electrically inactive. These are the first-principles physical counterpart of the chemical heuristic rules.

3.4. Donor Above Acceptor: Doping Type 1

In DT-1, for many different spinels calculated using DFT, we find that A^{3+}-on-T_d forms a donor in the gap located energetically above the B^{2+}-on-O_h acceptor, as shown in **Figure 4**. The donor-above-acceptor order of energy levels causes pinning ("locking") of the Fermi level via compensation, as explained above and shown in Figure 2a. Such Fermi level locking, however, does not mean that there could be no free carriers. The balance of carriers, whether n-type prevails over p-type or vice versa, depends critically on the relative concentration of the two anti-sites and on the position of their energy levels with respect to the band edges. We distinguish the following generic behaviors:

i) If the number of the A^{3+}-on-T_d donors and B^{2+}-on-O_h acceptors are comparable than: a) one expects net n-type behavior as exemplified by materials like In_2CdO_4 and Ga_2ZnO_4 (Figure 4) if the donor level lies closer to the CBM than the acceptor level is to the VBM. These are n-type compensated spinels. b) If the acceptor level lies closer to VBM than the donor level is to the CBM, signaling that the energy to ionize the acceptor is smaller than that needed to ionize the donor, (a case we call DT-1(p)), and exemplified by Co_2FeO_4, a net p-type behavior might be expected. We call these materials p-type compensated spinels. c) Finally, if the donor level position of the CBM is approximately equal to the acceptor level position of the VBM and if they lie either around the band edges, as exemplified by Al_2MgO_4 and Sc_2CdO_4, or at the mid gap, exemplified by Fe_2CoO_4, we have an electrically inactive intrinsic compensated spinel.

ii) However, if the number donor defects far exceeds the number of acceptors: a) net n-type behavior is expected when the donor is shallow, as exemplified by Fe_2ZnO_4, Fe_2MgO_4 and In_2MnO_4, or even if it is relatively deep compared to the acceptor; b) net insulating behavior is expected when donor is really deep; and similarly, if the number of acceptors far exceeds the number of donors, then: c) net p-type behavior is expected when the acceptor is shallow, as exemplified by In_2FeO_4 and Ga_2FeO_4, or if it is relatively deep compared to the donor, as exemplified by Ga_2FeO_4; and d) insulating behavior is expected when acceptor is really deep as exemplified by Ga_2MnO_4 and Sc_2MnO_4.

n-Typeness in this family of compounds can be enhanced by growing the compounds in an A-rich environment, as it promotes A substituting B in T_d sites, creating electrons. Similary p-typeness can be enhanced by growing the compounds in a B-rich environment, as it promotes B substituting A in O_h sites, creating holes. Furthermore, extrinsic doping in these spinels is unlikely to be effective:

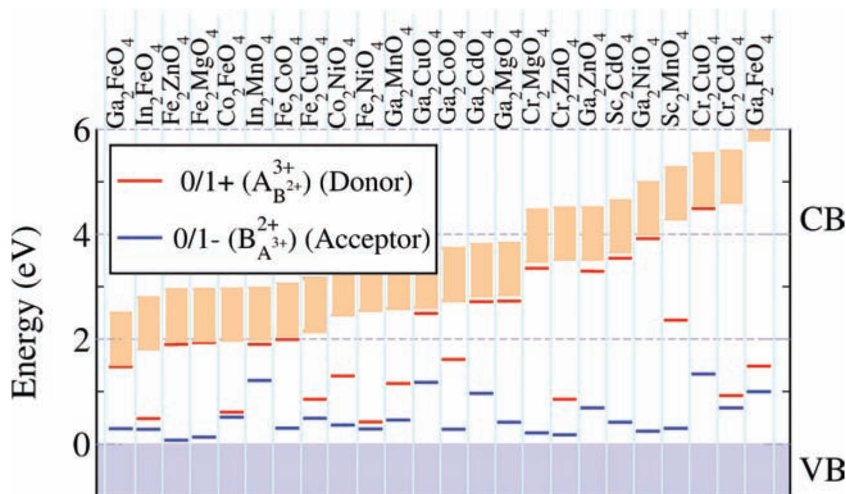

Figure 4. Calculated anti-site transition levels in various spinel oxides belonging to class DT-1. The VBM of each of the compound is set to zero in the plot.

© 2011 WILEY-VCH Verlag GmbH & Co. KGaA, Weinheim

i) If the Fermi level pinning occurs inside the gap as shown in many spinels including Al_2MgO_4, Ga2ZnO$_4$, and Ga_2CdO_4 (crossing of donor and acceptor formation energies, cf., Figure 2), the intrinsic compensating anti-site defect forms spontaneously and annihilates the effect of extrinsic doping.
ii) If the Fermi level pinning occurs inside the conduction or valence band, the intrinsic doping is already large and extrinsic doping is less relevant.

Overall, theoretically, DT-1 spinels have both donor and acceptor anti-sites levels in the gap in a specific order, as discussed above. They can be n-type, p-type, or insulating, and external doping would have a limited effect on the carrier concentration due to Fermi level pinning. Heuristically, spinels belonging to this group are distinguished by two cations that preserve their valences irrespective of the lattice sites they are on. Examples of such cations are A^{3+} = Al, Ga, In, and B^{2+} = Mg, Zn, Cd.

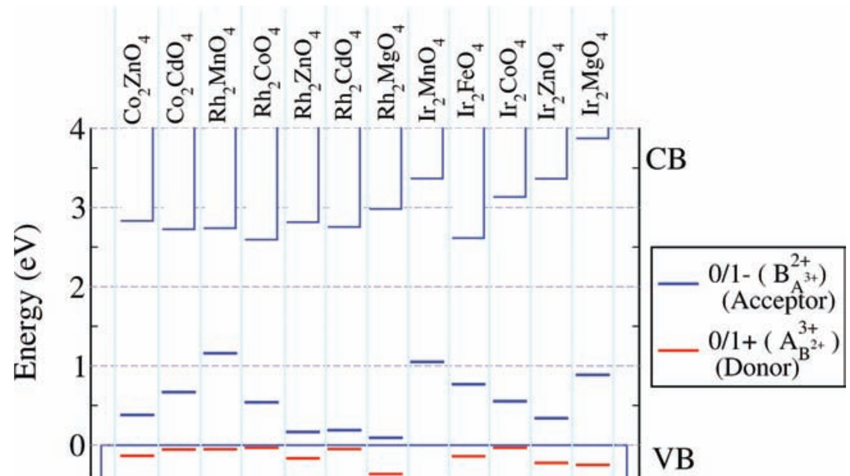

Figure 5. Calculated anti-sites transition levels for various spinel oxides of DT-2. The VBM of each of the compound is set to zero in the plot.

3.5. Acceptor Above Donor: Doping Types 2, 3, and 4

In DT-2, DT-3, and DT4, the Fermi level is not locked to a narrow region, because one of the defect levels is unable to compensate the other on account of its ionization energy being, for example, resonant within the continuum of energy states, and thus the defect is electrically inactive.

i) In DT-2 (p), the A^{3+}–on-T_d donor lies not only below the acceptor, but the donor is actually resonant within the valence band, as shown in **Figure 5**. Materials with high-lying VBM energies (relative to vacuum), such as those that have nonbonding character of the VBM, are more likely to show DT-2 behavior where the donor is swamped by the valence band. Such materials are likely to be good p-type conductors. In DT-2, B^{2+}-on-O_h is a hole-producing acceptor, unopposed by a compensating donor. Heuristically, materials with A on T_d sites are electrically inactive and could correspond to A-cations that are 3+ on their O_h home-site but become effectively 2+ on the T_d site without donating the difference charge to the conduction band. This effect was recently experimentally studied on the example of Co in Co_2ZnO_4.[47]
ii) In DT-3 (n) the B^{2+}-on-O_h acceptor level is not only above the donor level, but is actually resonant in the conduction band. Thus, A^{3+}-on-T_d is an electron-producing donor, unopposed by a compensating acceptor. Materials with low-lying CBM (relative to vacuum), such as indium-containing materials, are more likely to be DT-3, as the conduction band can swamp the acceptor level. Heuristically, materials with B-on-O_h being electrically inactive could correspond to B-cations that are 2+ on their T_d home site but become effectively 3+ on the O_h sites. First-principles calculations were so far unable to find rigorous examples of DT-3 (n) within the spinels studied here, even within the indium-based spinels. The reason is probably that in wide band gap semiconductors, such as spinels, it is difficult to find materials with acceptor states that are sufficiently high in energy to be resonant with the conduction band. If such a spinel with a low-lying CBM can be identified, it would be very good n-type conductor.
iii) In DT-4 both donor and acceptor levels are very deep, in fact so deep that the donor level lies below the acceptor level and that both of them are far from the corresponding band edges. Results of the first principles calculations are shown in **Figure 6** and illustrate some DT-4 cases. This behavior leads to no electrical compensation and unrestricted movement of the

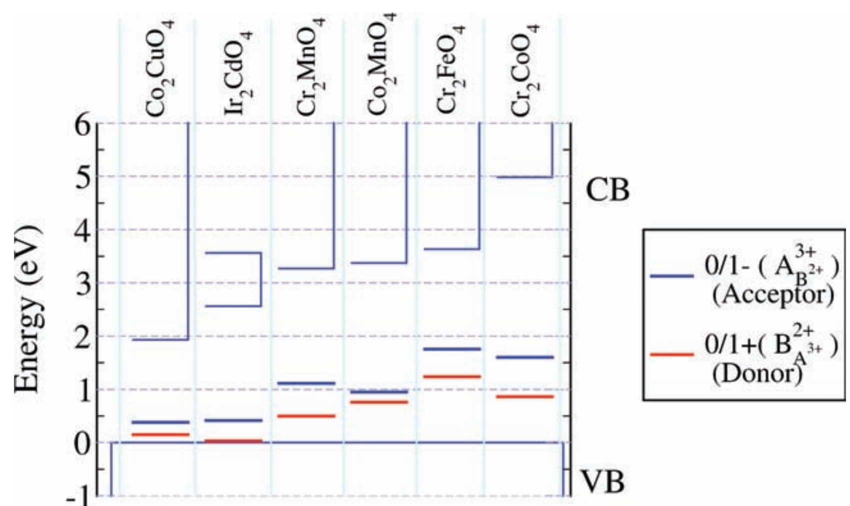

Figure 6. Calculated anti-site transition levels of various spinel oxides of the DT-4. The VBM of each of the compound is set to zero in the plot. Note that in Ir_2CdO_4 and Co_2CuO_4 the donor level lies just below the acceptor level, close to VBM. They indeed are the borderline compounds and could easily be either DT-2, if donor levels would be slightly deeper and fall below VBM, or DT-1, if the donor level would be slightly shallower and lie above the acceptor level.

© 2011 WILEY-VCH Verlag GmbH & Co. KGaA, Weinheim

Fermi level, as shown in Figure 2b, and such materials could in principle be doped both n- and p-type. Heuristically, DT-4 behavior is expected when both A^{3+} and B^{2+} atoms switch their oxidation states to 2+ and 3+, when moved to T_d and O_h sites, respectively.

4. Conclusion

By using first-principle defect calculation in a high-throughput manner, we show that the anti-site defects control the electrical properties in A_2BO_4 spinels. We systematize them according to their transitions levels and found rules that determine the doping in the spinel. We found that spinel oxides can be categorized into four doping types (DTs): i) the donor-above-acceptor type in which both are in the gap, i.e., both are electrically active and compensated (DT-1); ii) the acceptor-above-donor type in which only the acceptor is in the gap, i.e., only the acceptor is electrically active (DT-2); iii) the acceptor-above-donor type in which only the donor is in the gap, i.e., only the donor is electrically active (DT-3); and iv) the acceptor-above-donor type in which both are in the gap, i.e., both donor and acceptor are electrically active but not compensated (DT-4). External doping in the DT-1 materials leads to compensation, whereas in DT-2, DT-3, and DT-4 it lead to enhancement in number of carriers upon doping with the suitable dopants. These simple classification combined with the information about the response of system to the external doping provide a simple way to design a material with desired electrical properties.

Acknowledgements

This work was supported through the Center for Inverse Design, an Energy Frontier Research Center funded by the U.S. Department of Energy, Office of Science, Basic Energy Sciences. We thank Xiuwen Zhang for sharing an unpublished elemental chemical potential table and Vladan Stevanovic for important input and useful discussions.
Please note: This article was amended on December 6, 2011 to replace Figures with color versions.

Received: June 30, 2011
Revised: August 9, 2011
Published online: October 24, 2011

[1] Another widely used way of writing the spinel chemical formula is AB_2O_4. Here, we choose to use A_2BO_4 following Zhang and Zunger[2] mainly because the work presented here is part of a larger project that treats all A_2BX_4 compounds (not only spinels) in different structure types including olivine Fe_2SiO_4, β-K_2SO_4, and La_2CuO_4 for which A_2BX_4 is the generally used notation. Further it is to be noted that the A_2BO_4 notation is common for spinels with formal cation valencies $Z_A = 2$ and $Z_B = 4$, such as Mg_2TiO_4.[65]
[2] X. Zhang, A. Zunger, *Adv. Funct. Mater.* **2010**, *20*, 1944.
[3] R. J. Hill, J. R. Craig, G. V. Gibbs, *Phys. Chem. Miner.* **1979**, *4*, 317.
[4] Y. Yamasaki, S. Miyasaka, Y. Kaneko, J.-P. He, T. Arima, Y. Tokura, *Phys. Rev. Lett.* **2006**, *96*, 207204.
[5] P. Baltzer, H. Lehmann, M. Robbins, *Phys. Rev. Lett.* **1965**, *15*, 493.
[6] I. Hase, S.-ichi Ikeda, N. Shirakawa, J. K. Stalick, *J. Low Temp. Phys.* **2003**, *131*, 269.
[7] Y. Ishida, T. Baba, R. Eguchi, M. Matsunami, M. Taguchi, A. Chainani, Y. Senba, H. Ohashi, Y. Okamoto, H. Takagi, S. Shin, *Phys. Rev. B* **2009**, *80*, 081103.
[8] S. Yamanaka, H. Kobayashi, K. Kurosaki, *J. Alloys Compd.* **2003**, *349*, 321.
[9] Y. Fujishiro, K. Hamamoto, O. Shiono, S. Katayama, M. Awano, *J. Mater. Sci. Mater. Electron.* **2004**, *15*, 769.
[10] M. Isobe, M. Arai, E. Takayama-Muromachi, *J. Electron. Mater.* **2009**, *38*, 1166.
[11] N. K. Nga, K. C. Dang, *Adv. Tech. Mater. Mater. Process.* **2004**, *6*, 336.
[12] J. R. Scheffe, J. Li, A. W. Weimer, *Int. J. Hydrogen Energy* **2010**, *35*, 3333.
[13] N. Ueda, T. Omata, N. Hikuma, K. Ueda, H. Mizoguchi, T. Hasimoto, H. Kawazoe, T. Hashimoto, *Appl. Phys. Lett.* **1992**, *61*, 1954.
[14] T. Omata, N. Ueda, N. Hikuma, K. Ueda, H. Mizoguchi, T. Hashimoto, H. Kawazoe, *Appl. Phys. Lett.* **1993**, *62*, 499.
[15] T. Omata, N. Ueda, K. Ueda, H. Kawazoe, *Appl. Phys. Lett.* **1994**, *64*, 1077.
[16] C. F. Windisch, K. F. Ferris, G. J. Exarhos, *J. Vac. Sci. Technol., A* **2001**, *19*, 1647.
[17] M. Miyakawa, R. Noshiro, T. Ogawa, K. Ueda, H. Kawazoe, H. Ohta, M. Orita, M. Hirano, H. Hosono, *J. Appl. Phys.* **2002**, *91*, 2112.
[18] D. R. Kammler, T. O. Mason, K. R. Poeppelmeier, *Chem. Mater.* **2000**, *12*, 1954.
[19] S. E. Dorris, T. O. Mason, *J. Am. Ceram. Soc.* **1998**, *71*, 379.
[20] N. Mansourian-Hadavi, S. Wansom, N. H. Perry, A. R. Nagaraja, T. O. Mason, *Phys. Rev. B* **2010**, *81*, 021903.
[21] Z. Lu, J. Zhu, E. Andrew Payzant, M. P. Paranthaman, *J. Am. Ceram. Soc.* **2005**, *88*, 1050.
[22] A. Walsh, K.-S. Ahn, S. Shet, M. N. Huda, T. G. Deutsch, H. Wang, J. A. Turner, S.-H. Wei, Y. Yan, M. M. Al-Jassim, *Energy Environ. Sci.* **2009**, *2*, 774.
[23] A. Petric, H. Ling, *J. Am. Ceram. Soc.* **2007**, *90*, 1515.
[24] E. Zhecheva, R. Stoyanova, S. Angelov, *Mater. Chem. Phys.* **1990**, *25*, 351.
[25] E. Zhecheva, R. Stoyanova, S. Angelov, *Mater. Chem. Phys.* **1990**, *25*, 361.
[26] R. Stoyanova, E. Zhecheva, S. Angelov, *Mater. Chem. Phys.* **1990**, *26*, 239.
[27] Z. Łodziana, J. Piechota, *Phys. Rev. B* **2006**, *74*, 184117.
[28] S. B. Zhang, S.-H. Wei, *Appl. Phys. Lett.* **2002**, *80*, 1376.
[29] R. Pandey, J. D. Gale, S. K. Sampath, J. M. Recio, *J. Am. Ceram. Soc.* **2004**, *82*, 3337.
[30] A. Walsh, Y. Yan, M. M. Al-Jassim, S.-H. Wei, *J. Phys. Chem. C* **2008**, *112*, 12044.
[31] H. Moriwake, I. Tanaka, F. Oba, Y. Koyama, H. Adachi, *Int. J. Quantum Chem.* **2003**, *91*, 208.
[32] N. Appandairajan, *J. Solid State Chem.* **1981**, *40*, 117.
[33] H. Mizoguchi, M. Hirano, S. Fujitsu, T. Takeuchi, K. Ueda, H. Hosono, *Appl. Phys. Lett.* **2002**, *80*, 1207.
[34] F. Tinjod, P. de Mierry, D. Lancefield, Z. Bougrioua, S. Laügt, O. Tottereau, P. Lorenzini, S. Chenot, E. Virey, M. R. Kokta, J. L. Stone-Sundberg, D. Pauwels, *J. Cryst. Growth* **2005**, *285*, 450.
[35] M. Dekkers, G. Rijnders, D. H. A. Blank, *Appl. Phys. Lett.* **2007**, *90*, 021903.
[36] S. Kumar, R. Kumar, B. H. Koo, H. Choi, D. U. Kim, C. G. Lee, *J. Ceram. Soc. Jpn.* **2009**, *117*, 689.
[37] H. J. Kim, *J. Appl. Phys.* **2004**, *95*, 7387.
[38] S. E. Dorris, T. O. Mason, *J. Am. Ceram. Soc.* **1988**, *71*, 379.
[39] G. J. Exarhos, C. F. Windisch Jr., K. F. Ferris, R. R. Owings, *Appl. Phys. A* **2007**, *89*, 9.

© 2011 WILEY-VCH Verlag GmbH & Co. KGaA, Weinheim

[40] C.-J. Ting, H.-Y. Lu, *J. Am. Ceram. Soc.* **2004**, *82*, 841.
[41] R. J. Bratton, *J. Am. Ceram. Soc.* **1969**, *52*, 417.
[42] For example occupying 8b(3/8, 3/8, 3/8) position with metal ion(M), the two- coordination shells will be M-(A_4O_4)($A_{12}B_4$). Similarly, occupying 16c(0,0,0), leads to a M-(B_2O_6)(A_6) coordination shell. Other lower-symmetry Wyckoff positions convert themselves to high symmetry Wyckoff positions for certain values of *x*,*y*,*z*, and high-symmetry Wyckoff positions other then 8a, 16d lead to nonideal bonding and are unlikely to produce favorable bonding leading to occupation of interstitial positions.
[43] S. Lany, A. Zunger, *Phys. Rev. Lett.* **2007**, *98*, 7025.
[44] R. Dieckmann, H. Schmalzried, *Ber. Bunsen Ges. Phys. Chem.* **1977**, *81*, 344.
[45] R. Dieckmann, H. Schmalzried, *Ber. Bunsen Ges. Phys. Chem.* **1977**, *81*, 415.
[46] T. Paudel, S. Lany, M. D'Avezac, A. Zunger, N. Perry, A. Nagaraja, T. Mason, J. Bettinger, Y. Shi, M. Toney, *Phys. Rev. B* **2011**, *84*, 064109.
[47] J. D. Perkins, T. R. Paudel, A. Zakutayev, P. Ndione, P. A. Parilla, S. Lany, D. S.Ginley, Y. Shi, J. S. Bettinger, M. F. Toney, *Phys. Rev. B* **2011**, in press.
[48] S. Lany, A. Zunger, *Phys. Rev. B* **2008**, *78*, 016401.
[49] K. Biswas, S. Lany, *Phys. Rev. B* **2009**, *80*, 115206.
[50] H. Kamisaka, K. Yamashita, *J. Phys. Chem. C* **2011**, *115*, 8265.
[51] W. Chen, C. Tegenkamp, H. Pfnür, T. Bredow, *Phys. Rev. B* **2010**, *82*, 104106.
[52] S. J. Clark, J. Robertson, *Phys. Stat. Sol. B* **2011**, *248*, 537.
[53] J. Robertson, S. Clark, *Phys. Rev. B* **2011**, *83*, 075205.
[54] D. Huang, Y.-J. Zhao, D.-H. Chen, Y.-Z. Shao, *J. Phys. Condens. Matter* **2009**, *21*, 125502.
[55] S. Lany, A. Zunger, *Modell. Simul. Mater. Sci. Eng.* **2009**, *17*, 084002.
[56] H. Raebiger, S. Lany, A. Zunger, *Phys. Rev. B* **2009**, *79*, 165202.
[57] S. Lany, J. Osorio-Guillén, A. Zunger, *Phys. Rev. B* **2007**, *75*, 1203(R).
[58] M. Leslie, N. J. Gillan, *J. Phys. C* **1985**, *18*, 973.
[59] G. Makov, M. C. Payne, *Phys. Rev. B* **1995**, *51*, 4014.
[60] S. Baroni, R. Resta, *Phys. Rev. B* **1986**, *33*, 7017.
[61] T. S. Moss, *Proc. Phys. Soc. B* **1954**, *67*, 775.
[62] E. Burstein, *Phys. Rev.* **1954**, *93*, 632.
[63] T. R. Paudel, W. R. L. Lambrecht, *Phys. Rev. B* **2008**, *78*, 085214.
[64] V. Stevanović, M. D'Avezac, A. Zunger, *Phys. Rev. Lett.* **2010**, *105*, 075501.
[65] B. A. Wechsler, A. Navrotsky, *J. Solid State Chem.* **1984**, *55*, 165–180.

© 2011 WILEY-VCH Verlag GmbH & Co. KGaA, Weinheim